Pol. J. Environ. Stud. Vol. XX, No. X (XXXX), 1-14
DOI: *10.15244/pjoes/209834* ONLINE PUBLICATION DATE: 2025-09-25

Original Research

Integrating Geo-AI with GIS and RS for Analyzing Land Cover Transformation and Its Impacts in Henan

Zhenjiang Dong°*

Hebi Polytechnic, Hebi City, Henan, China

Received: 6 July 2025
Accepted: 23 August 2025

Abstract

Understanding the interaction between land use and land surface temperature (LST) is essential for tackling the increasing problems of urbanization, environmental degradation, and climate change. This research explores the spatial and temporal patterns of Land Use and Land Cover (LULC) and their effect on LST in Henan Province, China, between 1990 and 2024, spanning 34 years. Using multi-temporal Landsat imagery, supervised classification using the Random Forest algorithm, and cloud-based processing in Google Earth Engine (GEE), we have mapped LULC changes and extracted LST values with high spatial resolution and temporal consistency. The findings indicate extensive land transformation, with urban areas increasing by more than 181%, mainly at the cost of cropland, which decreased by almost 11%. Concurrently, LST rose markedly, with maximum surface temperatures increasing from 43.2ºC to 51.3ºC. Built-up and barren land exhibited the highest mean LST values, while forests and water bodies consistently recorded cooler temperatures, highlighting the role of vegetative cover and hydrological features in mitigating surface heat. To quantify these relationships, Pearson correlation analysis was performed between the area of each LULC class and its corresponding LST. The results showed significant positive correlations between land built-up and LST ($r>0.94$), and significant negative correlations for cropland and forest cover ($r<-0.95$), affirming the urbanization- and land-degradation-related thermal amplification. The research establishes the pivotal relationship between LULC changes and surface thermal trends, providing an actionable geospatial model for environmental monitoring and land management. The incorporation of long-term satellite data with statistical correlation produces actionable information for policymakers, urban planners, and sustainability stakeholders. With Henan and much of the rest of the world continuing to urbanize rapidly, this study reinforces the need to balance development with ecological resilience to reduce increasing surface temperatures and their larger climate impacts.

Keywords: remote sensing, urban heat island, climate change, land management, sustainability

*e-mail: dongzhenjiang@hbzy.edu.cn
°ORCID iD: 0000-0002-2540-391X

Introduction

In recent decades, rapid urbanization and changes in land use have significantly altered the landscapes around the world. One of the most noticeable outcomes of these changes is the increase in land surface temperature (LST), especially in urban areas where natural vegetation has been replaced by built-up surfaces like concrete and asphalt [1]. These changes not only disrupt the natural energy balance at the surface but also contribute to the urban heat island (UHI) effect, which can intensify local climate conditions, increase energy consumption, and pose health risks in densely populated areas [2].

LST is a valuable indicator for studying how changes in land use and land cover (LULC) affect surface temperature. It reflects the combined influence of factors such as vegetation cover, surface materials, soil moisture, and human activities. Although many studies have explored the link between urban growth and rising surface temperatures [3, 4], there is still a need for long-term, high-resolution analysis at regional levels, especially in places like inland China, where urbanization is advancing rapidly but unevenly [5].

Land Surface Temperature (LST) is a crucial, quantifiable indicator of environmental change. LST captures the effects of numerous surface characteristics, including albedo, vegetation density, moisture conditions, and anthropogenic heat discharge. Many empirical studies have repeatedly demonstrated that LULC changes, particularly the expansion of agricultural or forest land to urban areas, correlate strongly with increases in LST values. This effect, referred to as the Urban Heat Island (UHI) phenomenon, is marked by increased urban temperatures above those in the rural environment because of concentrated infrastructure and minimal vegetation [5]. The UHI effect leads to a cascade of secondary issues, including higher cooling energy consumption, higher air pollution levels, threats to rare and endemic species [6], and more severe public health threats associated with heat stress and cardiovascular conditions.

Henan Province, located in central China, offers a compelling case for such an investigation. With over 99 million residents, Henan has undergone major shifts in land use patterns over the past three decades. What was once a largely agricultural landscape has increasingly been converted into urban and industrial zones. While several national and city-level studies have looked at these trends [7], Henan's transformation has not yet been examined in detail using advanced remote sensing and machine learning tools that can capture spatial and temporal changes at a finer scale.

This study aims to fill that gap by analyzing the evolution of LULC and its impact on LST in Henan from 1990 to 2024. We use Landsat satellite imagery and Google Earth Engine (GEE) to map land cover changes, applying the Random Forest (RF) algorithm to classify different land types. LST is retrieved using the Radiative Transfer Equation method, and we explore the relationships between land cover types and their corresponding surface temperatures over time. This approach allows us to examine not only how the landscape has changed but also how these changes have influenced local temperature dynamics.

What sets this study apart is its combination of long-term satellite data, cloud-based processing, and machine learning classification to produce a high-resolution analysis of land-atmosphere interactions across a rapidly developing region. In addition to mapping LULC and LST changes, we also aim to distinguish between surface temperature changes caused by land cover shifts and those driven by broader climatic factors.

This study contributes to a deeper understanding of how human-driven land transformation is shaping thermal environments in inland China. It also offers practical insights for urban planners and policymakers working to design more climate-resilient cities in the face of ongoing development.

Materials and Methods

Study Area

Henan Province, located in central China, covers an area of around 167,000 km^2 and sits at the heart of the North China Plain (Fig. 1). It is bordered by several provinces: Shandong to the east, Shaanxi to the west, Hebei to the north, and Hubei to the south, making it a central hub in the country's geography, economy, and culture. The landscape is mostly flat in the central and eastern parts, where fertile plains dominate, while the western and southern regions are more mountainous and forested [8].

Henan experiences a temperate monsoon climate with four distinct seasons. Summers are typically hot and humid, and winters are cold and dry. The average annual temperature ranges from 12ºC to 16ºC, and most rainfall falls between June and September. These seasonal patterns, along with the province's varied topography, influence both land use practices and surface temperature patterns, factors that are central to this study.

Henan is one of China's most populous provinces, with more than 99 million residents. Historically, it has been a major agricultural region, often referred to as the "breadbasket" of China. In recent decades, however, Henan has experienced rapid urbanization and economic growth [9]. Cities like Zhengzhou (the capital), Luoyang, Kaifeng, and others have expanded significantly, with rural land increasingly being converted to urban and industrial uses.

This transformation has brought both opportunities and challenges. On one hand, urban growth has spurred infrastructure development and improved livelihoods for many. On the other hand, it has placed pressure on farmland, water resources, and natural ecosystems. These changes also have important implications for land

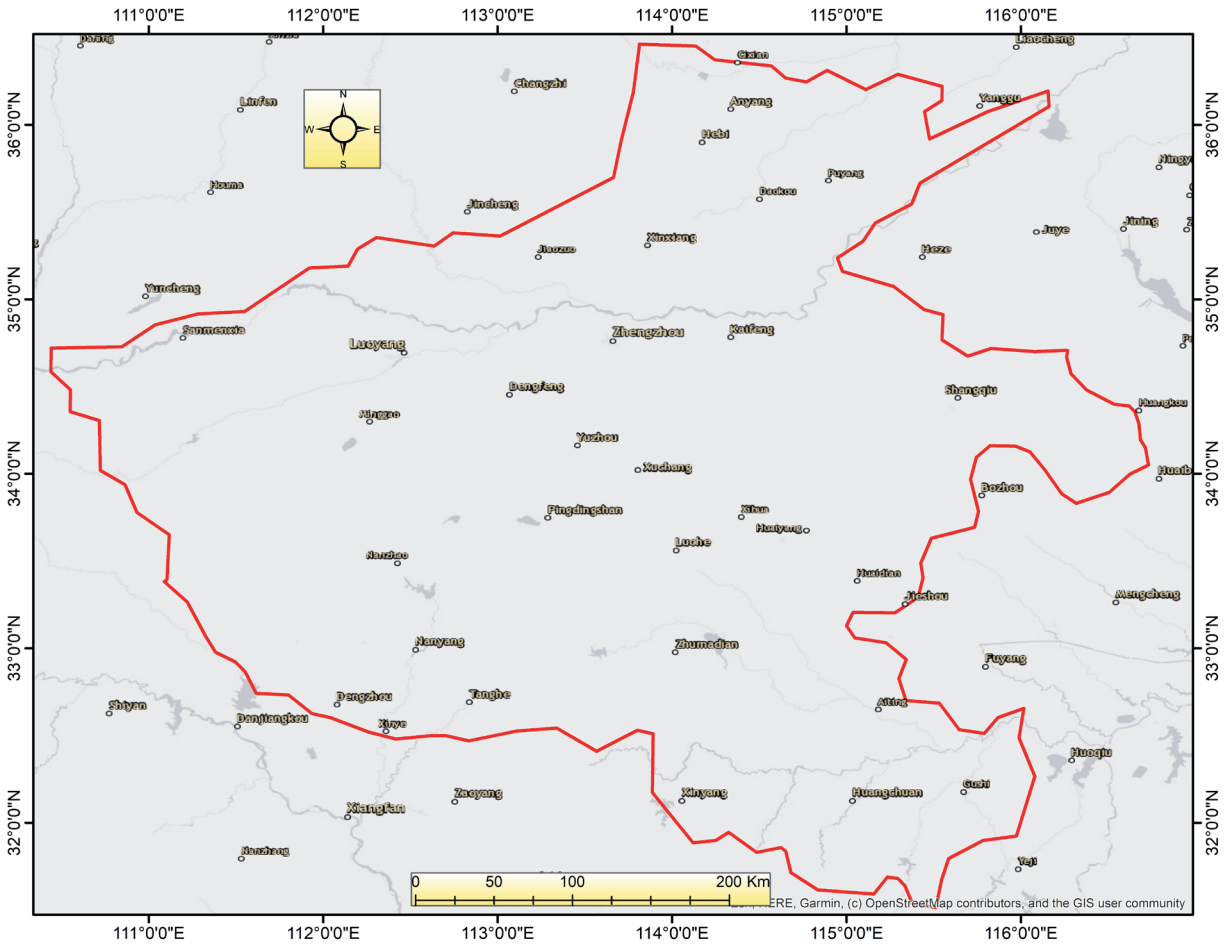

Fig. 1. Study Are map of Henan Province, China, showing administrative boundries, major cities, and the provincial position within China.

surface temperature, especially as natural vegetation gives way to impervious urban surfaces that absorb and retain more heat.

Henan's mix of urban growth, agricultural heritage, and ecological zones makes it a strong case for studying the relationship between LULC and LST [10]. The province offers a valuable setting to observe how different land cover types, from croplands and forests to built-up and barren areas, respond thermally to human activities and development pressures. By focusing on Henan, this research aims to generate insights that are not only locally meaningful but also relevant to other regions facing similar transitions [8].

Data Acquisition and Preprocessing

To assess long-term LULC and LST changes, we used multi-temporal cloud-free Landsat imagery from five representative years: 1990, 2000, 2010, 2020, and 2024. The images were accessed using Google Earth Engine (GEE), Landsat 5 TM, Landsat 7 ETM+, and Landsat 8 OLI/TIRS, depending on availability for each time point.

All images were selected from the same season, preferably summer (June to August), to reduce seasonal variability and ensure comparability. This is particularly important in LST analysis, where surface heating varies significantly across seasons. Image preprocessing was conducted on the GEE platform and included:

- Top-of-atmosphere (TOA) correction, to standardize radiometric values;
- Cloud and shadow masking, using the QA_PIXEL quality band;
- Image mosaicking and compositing, where needed, to fill gaps;
- Resampling of thermal bands to match the 30-meter resolution of the visible bands for consistent analysis.

We prioritized image quality by filtering based on cloud cover percentages and selecting the best-scene composites when multiple images were available. Only scenes with minimal cloud contamination (<10%) were retained.

Land Use/Land Cover Classification

For LULC classification, we used the Random Forest (RF) algorithm, a widely used and robust machine learning method that handles high-dimensional data effectively and avoids overfitting (Fig. 2). The classification was performed in GEE, which

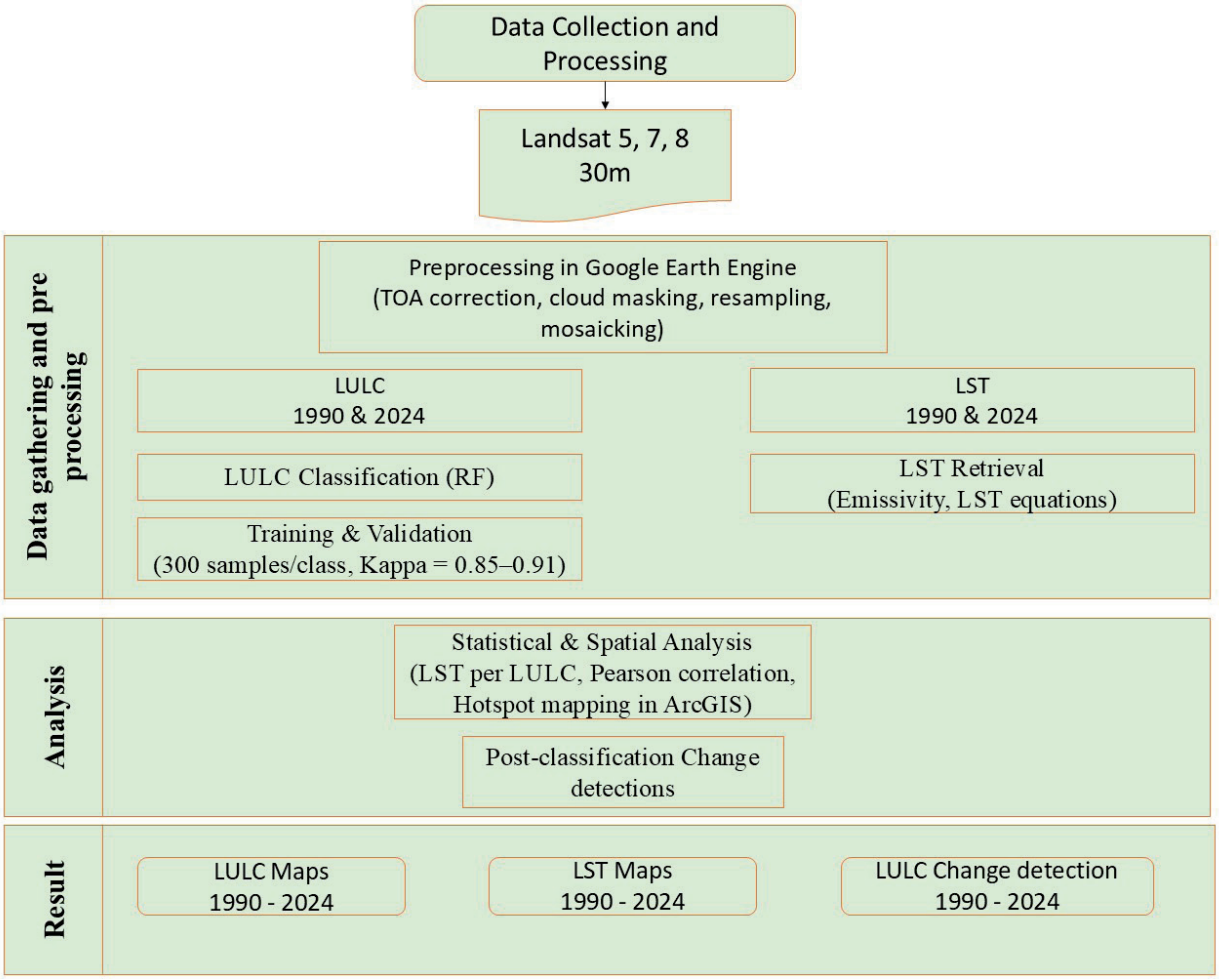

Fig. 2. Flow chart of the methodological framework, illustrating data acquisition, processing, land use land cover classification, land surface temperature retrieval and statistical analysis steps.

allowed for efficient processing of large-scale satellite datasets over the multi-decadal timeframe [11]. Seven major land cover classes were defined based on visual inspection, local knowledge, and literature: Cropland, Forest, Rangeland, Water Bodies, Built-up Area, Barren Land, and Snow/Ice.

Training and Validation

Training samples were manually selected from each year using high-resolution base maps in Google Earth. For each LULC class, approximately 300 training samples were collected, ensuring spatial and thematic representation across the province. Samples were distributed to capture variation across urban, rural, and natural areas. Roughly 70% of the samples were used for training the model, while 30% were retained for accuracy assessment.

Classification accuracy was evaluated using confusion matrices and the Kappa coefficient, which ranged from 0.85 to 0.91 across the five years, indicating high reliability of the classified maps. Detailed accuracy results and class-wise performance are presented in the results section. Cross-validation was also applied to test classification robustness across years and classes.

Change Detection Analysis

To track how LULC evolved, we performed post-classification change detection. This method compares classified land cover maps across different years to identify transitions (e.g., cropland to built-up area). We generated transition matrices and spatial change maps that highlight major land conversions [12]. This helped quantify both the extent and direction of change, which is critical for understanding which land types are being lost or gained. Change statistics were calculated in square kilometers, and percentage changes were derived to assess gains or losses for each class between 1990 and 2024.

Land Surface Temperature (LST) Retrieval

In this study, Land Surface Temperature (LST) was retrieved from Landsat thermal imagery using the Radiative Transfer Equation (RTE) approach in Google

Earth Engine (GEE) [13]. This method was chosen for its physical reliability and compatibility with single-band thermal sensors, such as those onboard Landsat 5 TM, Landsat 7 ETM+, and Landsat 8 TIRS (Band 10). Since some Landsat missions do not offer two thermal bands, the Split-Window technique was not used [14]. The LST retrieval process included the following steps:

First, raw digital number (DN) values from the thermal band were converted to Top-of-Atmosphere (TOA) spectral radiance using radiometric rescaling factors provided in the metadata:

$$L\lambda = ML \times Qcal + AL$$

Where:
- Lλ: TOA spectral radiance (W/m²·sr·μm)
- Qcal: Quantized and calibrated pixel value (DN)
- ML: Radiance multiplicative scaling factor
- AL: Radiance additive scaling factor

The TOA radiance values were then converted to brightness temperature (BT) in Kelvin using the inverse Planck function:

$$T\_sensor = K2 / \ln(K1 / L\lambda + 1)$$

Where:
- T_sensor: At-sensor brightness temperature.
- K1 and K2: Calibration constants (specific to each Landsat sensor, found in the metadata)

To adjust for differences in how various surfaces emit thermal radiation, land surface emissivity (ε) was estimated using the NDVI Thresholds Method (NTM). NDVI was calculated using the red and near-infrared bands, and emissivity was assigned based on NDVI values as follows:

$$\epsilon_\lambda = \begin{cases} \epsilon_s, & NDVI < NDVI_s \\ \epsilon_s P_v + \epsilon_s (1 - P_v) + C, & NDVI_s \leq NDVI \leq NDVI_v \\ \epsilon_s + C, & NDVI > NDVI_v \end{cases}$$

Where:
- εv = 0.985: Emissivity of vegetation
- εs = 0.960: Emissivity of bare soil
- C = 0.005: Correction factor for surface roughness
- NDVI_s = 0.2, NDVI_v = 0.5: Threshold values
- Pv = ((NDVI - NDVI_s) / (NDVI_v - NDVI_s))²: Proportion of vegetation

With the emissivity and brightness temperature estimated, LST was computed using the Radiative Transfer Equation [13], which accounts for the effect of emissivity and corrects for atmospheric distortion:

$$LST = \frac{T_{\text{sensor}}}{1 + \left(\frac{\lambda \cdot T_{\text{sensor}}}{\rho}\right) \cdot \ln(\varepsilon)}$$

Where:
- LST: Land surface temperature (Kelvin)
- λ = 10.895 μm: Effective wavelength of the thermal band
- ln(ε) = accounts for how well the surface emits heat (lower emissivity = higher correction)

Finally, LST was converted from Kelvin to Celsius:

$$LST\ (°C) = LST - 273.15$$

Statistical and Spatial Analysis

To explore the relationship between land cover changes and surface temperature, we extracted the mean LST values for each LULC class in each year. This allowed us to compare how different land types (e.g., cropland vs. built-up) responded thermally over time. Pearson correlation was performed to quantify the strength and the direction of relationships between LULC area and mean LST values across the five study years. While correlation does not imply causation, this method provides a first-level statistical link between land transitions and temperature trends.

Spatial overlays, LST heat maps, and land cover change maps were generated using ArcGIS Pro for clearer visualization of hotspots and cold zones across the province. These visualizations helped highlight spatial clusters of surface heating, particularly in rapidly urbanizing areas.

Results

Over the past 34 years, Henan Province has undergone major changes in how its land was used and covered. The most dramatic shift was the rapid expansion of built-up areas, which grew from just over 9,000 km² in 1990 to more than 25,500 km² in 2024. That's an increase of around 485 km² per year, mostly around key urban centers like Zhengzhou and Luoyang.

Land Use Land Cover (LULC)

This urban growth came at the cost of cropland. Farmland shrank from roughly 170,500 km² to 151,900 km², which means Henan lost about 546 km² of cropland every year on average. That's a substantial loss in a province historically known as one of China's most important agricultural regions (Fig. 3).

Forest cover, on the other hand, remained mostly stable over the decades, fluctuating only slightly. Water bodies expanded by nearly 60%, likely due to new reservoirs and better detection through modern satellite imagery. There was also some growth in rangeland, while barren land, although still a small portion of the total area, increased significantly in percentage terms, possibly due to land degradation or construction activities.

Henan's landscape has been transformed, with cities spreading outward and farmland shrinking year by

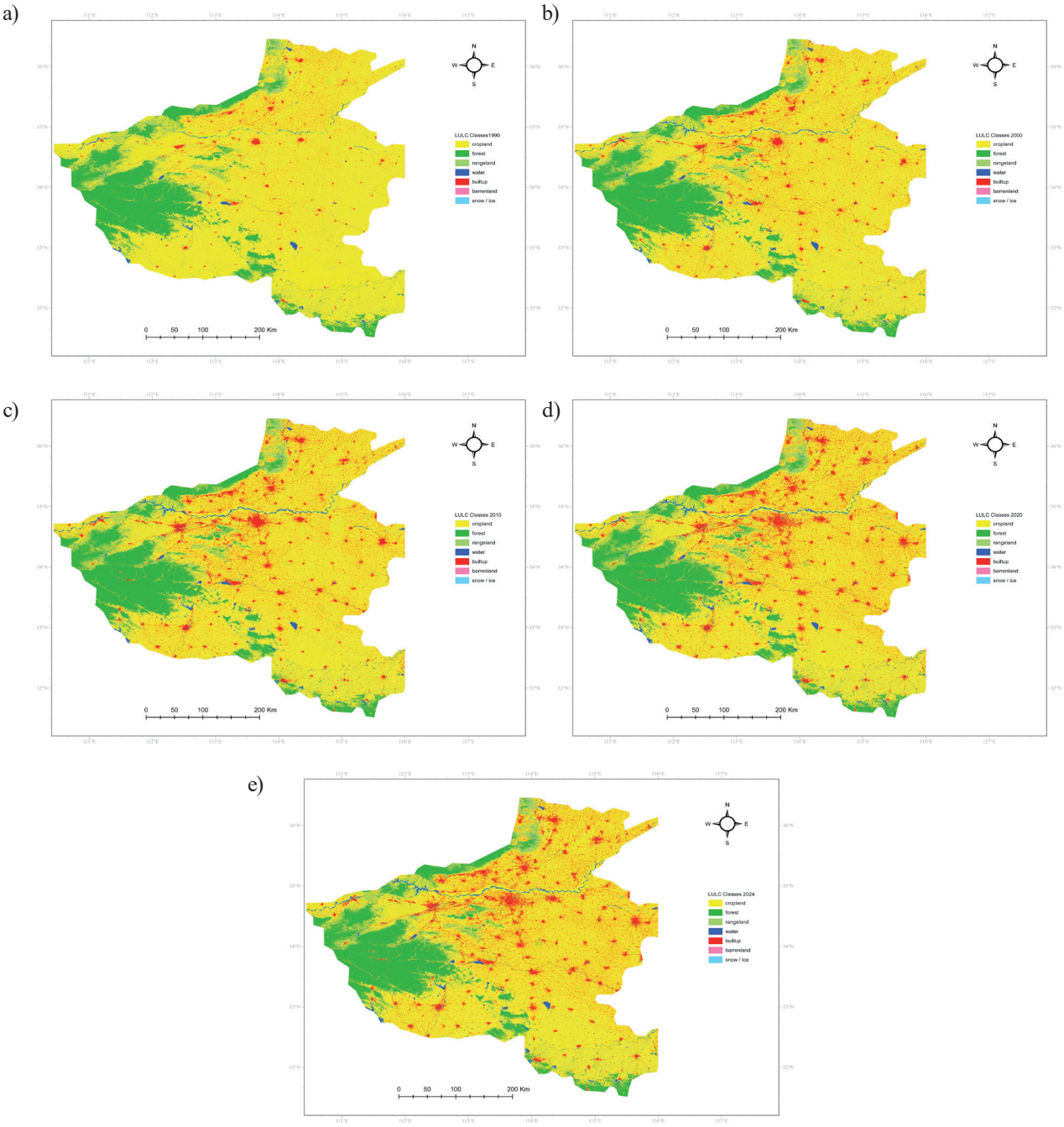

Fig. 3. LULC Maps of Henan Province. a) 1990, b) 2000, c) 2010, d) 2020, and e) 2024.

year. Forests have stayed mostly intact, while water and rangeland have grown gradually.

In general, the 34-year pattern of LULC change in Henan reflects a distinct story of urbanization at the cost of cropland, accompanied by relative forest conservation and stable water resources. These patterns underscore the imperative for sustainable land-use planning, reconciling economic growth with ecological and agricultural sustainability. In the future, strategic land management and environmental protection will be critical to counteract the effects of urban sprawl, conserve food security, and ensure regional ecosystem health.

Land Surface Temperature (LST)

Along with changes in land use, surface temperatures have also climbed. In 1990, the hottest areas in the province reached about 43.2ºC, but by 2024, that number had increased to 51.3ºC. That's a noticeable rise in just over three decades. Built-up and barren lands were consistently the hottest areas. Urban temperatures, on average, rose from around 34.8ºC to 40.5ºC, highlighting the well-known Urban Heat Island (UHI) effect, where cities trap more heat due to concrete, asphalt, and limited vegetation. Forests and water bodies remained the coolest areas throughout the study,

thanks to their ability to regulate temperature through shade and evapotranspiration. Cropland also had a cooling effect, though it has been warming over time, especially in areas where it was reduced or fragmented. As cities expanded, temperatures rose, especially in urban and bare areas. Vegetated regions like forests and croplands helped to keep things cooler, though their influence has weakened in places where they've declined (Fig. 4).

By 2010, LST increased further, at temperatures between 26.7ºC and 45.6ºC. Thermal contrast over the province became even greater, and extensive areas of high-temperature zones were seen in the western and southwest parts of the province, signifying enhanced urban sprawl as well as decreased vegetation cover. The year 2020 followed the same trend of warming, with surface temperature rising to 27ºC-48.1ºC (Fig. 4). While there were some isolated areas of cooler zones in the northeast and west, the majority of the province indicated heat stress, especially in areas of rapid urbanization and intensive agriculture.

The most profound thermal change happens in 2024, in which the range of LST hit a record high of 27.8ºC to 51.3ºC. The thermal landscape in the province grew dominated by expansive red and orange regions, illustrating extreme warming. This temperature jump is most seen in the center, east, and south zones, which now have widespread heat island effects thanks to the high concentration of built-up urban areas and few plants. Cooler areas have progressively fragmented and become restricted to the far west and northwest, which indicates a continued loss of ecological buffers.

In general, the progressive rise in maximum LST values from 43.2ºC in 1990 to 51.3ºC in 2024 reflects the important impact of anthropogenic activities on the thermal conditions of Henan Province. Urban sprawl, land degradation, and vegetation destruction have all been responsible for increasing surface temperatures. This growing trend in LST highlights the imperative need for sustainable land management, more green spaces in urban areas, and strategic planning to counter the impacts of heat stress and climate change in the region [15].

LULC Change Detection

The map of LULC (Land Use/Land Cover) change detection for Henan province from 1990 to 2024 indicates massive changes for different land types, demonstrating the dynamic interplay between nature and human activities for the last three decades. The most prominent change is the widespread expansion of built-up areas, particularly around urban centers and along transportation corridors. The deep red color, representing areas that were built-up in both 1990 and 2024, and the shades of brown and purple denoting transitions from cropland and forest to built-up, highlight extensive urbanization. This trend aligns with the broader socioeconomic development of the region, driven by population growth, industrialization, and infrastructural expansion (Fig. 5).

A considerable portion of the landscape, particularly in the central and eastern parts of Henan, is dominated by yellow patches labeled as cropland-to-cropland, indicating stable agricultural zones. However, surrounding these zones are scattered transitions from cropland to built-up areas, suggesting that farmland is increasingly being converted to accommodate urban development. This shift may have implications for food security and rural livelihoods, especially if not managed sustainably.

In the south/western mountainous and forested regions of Henan, the persistence of forest cover is apparent, shown by the dark green "forest-to-forest" class. However, there are also signs of encroachment, with patches showing transitions from forest to other land uses, including rangeland and built-up areas. These changes may be indicative of deforestation, possibly due to logging, agricultural expansion, or settlement spread.

Water bodies have undergone relatively minor changes, but some transitions are evident, particularly from water to built-up and water to cropland, which may reflect both natural drying or redirection of watercourses and human-led water reclamation or infrastructure projects.

Overall, the map underscores the dominant trend of urban expansion, the relative stability of core agricultural areas, and the moderate degradation or conversion of forested landscapes. These LULC dynamics have likely played a critical role in altering the land surface temperature (LST) of the region, as seen in the corresponding LST maps, emphasizing the link between land management, urban planning, and climatic variables.

The LULC changes of Henan from 1990 to 2024 have been analyzed, bringing forth clear variations in the spatial pattern of various classes. The most remarkable observation is the decrease in cropland, which has been reduced from about 170,467 km^2 in 1990 to 151,901 km^2 in 2024, representing a decrease of about 10.89%. This suggests that extensive tracts of agricultural land have probably been switched to other purposes, mostly urban and built-up land uses, indicating the area's increasing urbanization and infrastructural development (Table 1).

The forest cover, however, was incredibly resilient over the 34-year duration, growing modestly from 32,451.57 km^2 to 32,472.67 km^2, a 0.06% marginal increase. This indicates good forest management policies or minimal deforestation, which is good news for the environmental sustainability of the region. Likewise, rangelands have seen a modest 9.5% increase, perhaps resulting from natural regrowth in some regions or realignment from marginal agriculture to grasslands.

A greater increase is seen in waterbodies within which area increased from 2,114.15 km^2 in 1990 to 3,369.66 km^2 in 2024, an increase of 59.34%. This may be due to the construction of artificial reservoirs, enhancement in water conservation schemes,

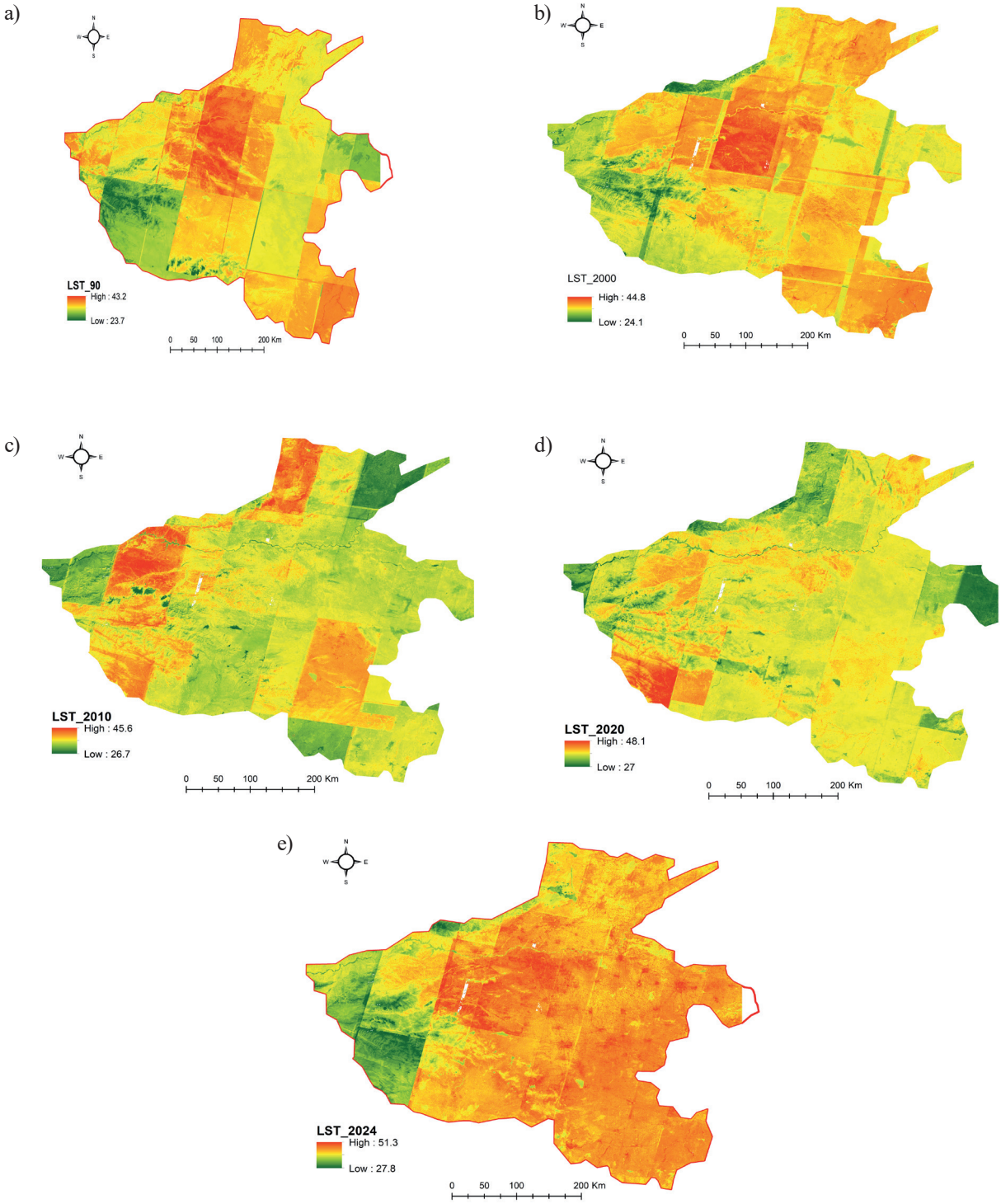

Fig. 4. LST Maps of Henan Province from 1990 to 2024.

or more advanced remote sensing detection technology in recent years. The surge in built-up areas is even more dramatic. From 9,096.34 km^2 in 1990 to 25,592.16 km^2 in 2024, the urban area has almost tripled, increasing by 181.24%. This reflects the region's fast rate of urban growth, which is probably due to population increase, economic growth, and land use change.

Although empty land remains a limited area, it has risen, skyrocketing from 5.85 km^2 to 99.8 km^2 by a whopping rise of 1606.08%. This might be an indicator of environmental degradation, enhanced soil erosion, or the land turning unfit for agriculture or vegetation. Finally, land covered with snow/ice, which was trivial in 1990 at 0.25 km^2, has grown to 11.81 km^2 as of 2024. This is a 4538.36% rise, which, although extreme in percent terms, would most probably represent improvements in detection of seasonal snow, increased altitudinal resolution in classification, or even

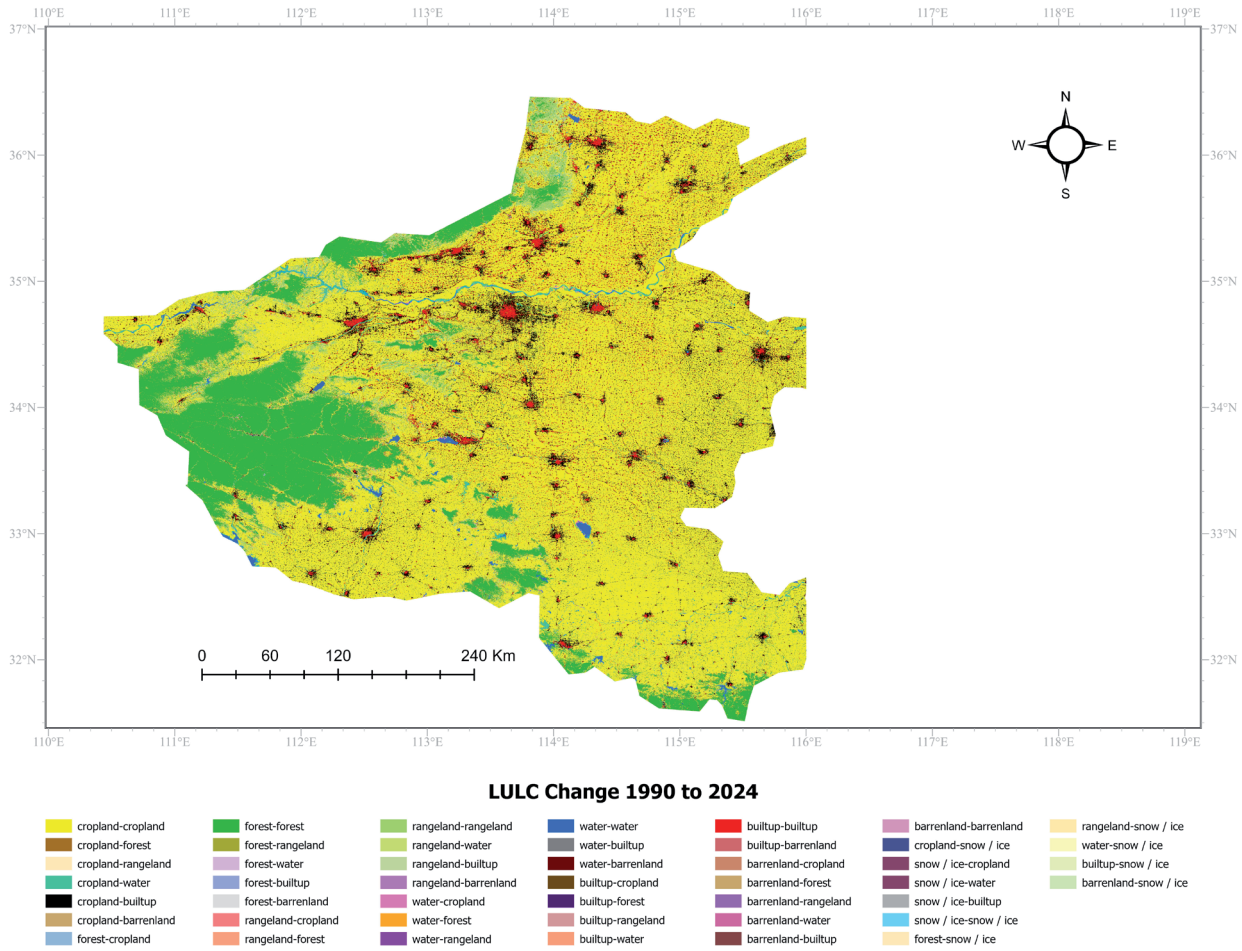

Fig. 5. Changes in LULC from 1990 to 2024.

Table 1. Area of each Land Use Land Cover (LULC) class (km^2), and percentage change from 1990 to 2024 in Henan Province, China.

LULC Classes	1990	2000	2010	2020	2024	% Change (1990-2024)
Cropland	170,467.24	160,945.90	156,126.68	151,959.42	151,900.81	−10.89%
Forest	32,451.57	32,471.82	32,186.73	32,484.09	32,472.67	0.06%
Rangeland	7,249.14	7,751.12	8,039.57	7,903.50	7,937.51	9.50%
Water	2,114.15	2,591.67	2,971.12	3,325.42	3,369.66	59.34%
Built-up	9,096.34	17,608.55	22,030.31	25,619.24	25,592.16	181.24%
Barrenland	5.85	3.67	18.29	80.95	99.8	1606.08%
Snow/Ice	0.25	11.85	11.81	11.81	11.81	4538.36%

modifications in local climatic conditions making snow cover visible (Fig. 6).

In general, the findings show a pronounced trend of urbanization, decreasing agricultural lands, and the occurrence of environmental alterations like expanding barren areas and water bodies. These trends indicate the necessity for sustainable land use planning and more research on the factors driving these changes.

Relationship between LULC and LST

The figure depicts the temporal trends in average Land Surface Temperature (LST) for all LULC classes in Henan Province from 1990 to 2024. The trend is clearly shown where urban areas always have the highest LST values, increasing from around 34.8ºC in 1990 to 40.5ºC in 2024, which is indicative of the growing urban heat island (UHI) effect as a result of increased impervious

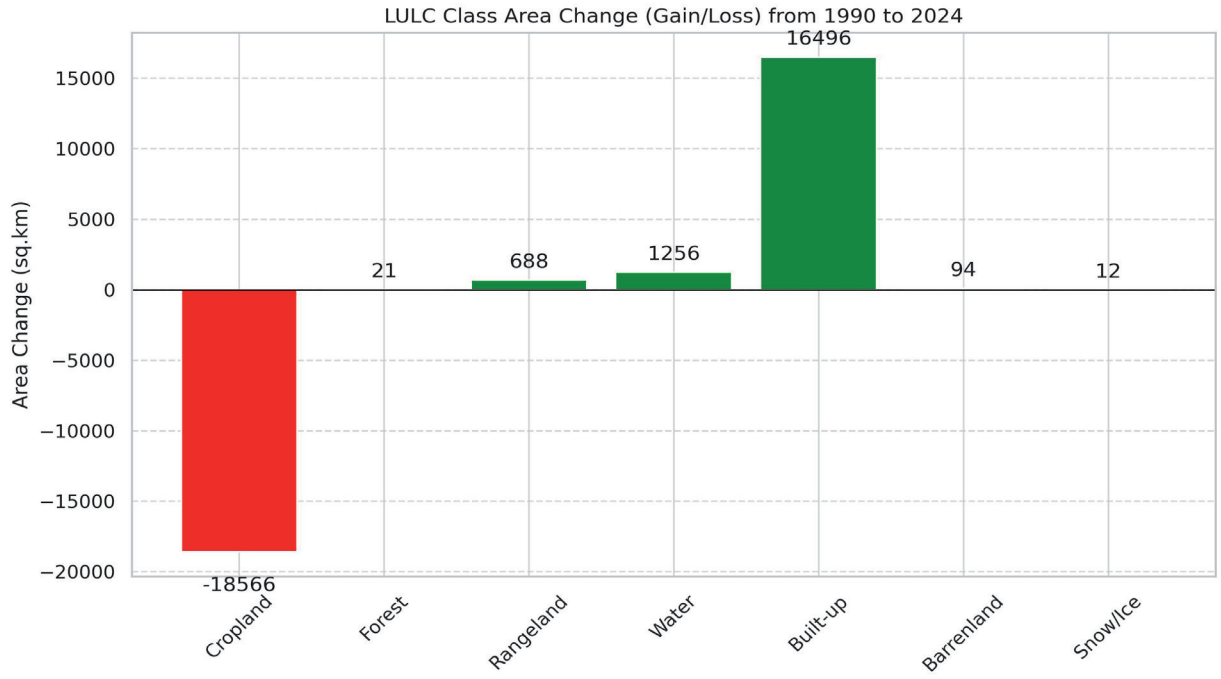

Fig. 6. LULC Class Area change (Gain/Loss) from 1990 to 2024.

surfaces and decreasing vegetation. Cropland and Rangeland also exhibit a significant increase in surface temperatures, to as high as 36.0ºC and 35.8ºC, respectively, by the year 2024. This indicates that farming and grazing areas are becoming increasingly warmer, perhaps because of vegetation deterioration or alteration in moisture levels and reflectance on the surface.

Forest covers, although with a modest rise, are considerably cooler across the duration, highlighting their pivotal function in thermal regulation and microclimate stability. Likewise, water bodies persistently show the lowest LST values, with an alluvial and steady increase, due to high heat capacity and evaporative cooling.

Interestingly, in 2024, there is a strong increase in LST on barren land that approaches the levels of built-up land use. This is because exposed, unvegetated surfaces tend to be heat-retaining. Snow/ice-covered areas, though minimally in extent, maintain the lowest overall temperatures, rising only slightly over time (Fig. 7).

Correlation Analysis between LULC and LST

To examine the statistical correlation of land use/land cover (LULC) changes and land surface temperature (LST), Pearson's correlation analysis was employed. The objective was to determine how alterations in the area of various land covers affect their corresponding thermal responses across periods. To achieve this, area information (in km^2) per LULC class and its respective mean LST (in degrees Celsius) were tabulated for the years 1990, 2000, 2010, 2020, and 2024.

Seven LULC classes were analyzed in the study: cropland, forest, rangeland, water bodies, built-up area, barren land, and snow/ice. For every class, the mean LST for every reference year was extracted from already processed thermal imagery. Area and LST datasets were merged into one multivariate data frame. Pearson's correlation coefficient (r) measured the association between the area of every land cover class and its corresponding LST for the five time points.

The correlation analysis revealed several key patterns. Most notably, a strong negative correlation was observed between the cropland area and its mean LST ($r = -0.96$). This suggests that as the area of cropland declined over time, surface temperatures in cropland zones rose significantly. This result aligns with the observed trend of cropland being increasingly converted into built-up land, which absorbs and retains more heat due to the lack of vegetative cover (Fig. 8).

In contrast, built-up land showed a very strong positive correlation with LST ($r \approx 0.94$-0.98), indicating that the expansion of urban and impervious surfaces is closely linked with rising land surface temperatures. This supports the well-documented urban heat island (UHI) effect and confirms that built-up zones in Henan are the most heat-vulnerable landscapes.

Rangeland and barren land also showed moderate to strong positive correlations with LST, suggesting that areas with exposed soil or degraded vegetation experience higher heat accumulation. Barren land displayed a rising area and increasing LST simultaneously, reflecting both environmental degradation and reduced surface albedo. Forest area, despite remaining relatively stable over the 34 years, showed a very weak or no correlation with LST ($r = 0.09$). This suggests that forests, due to their

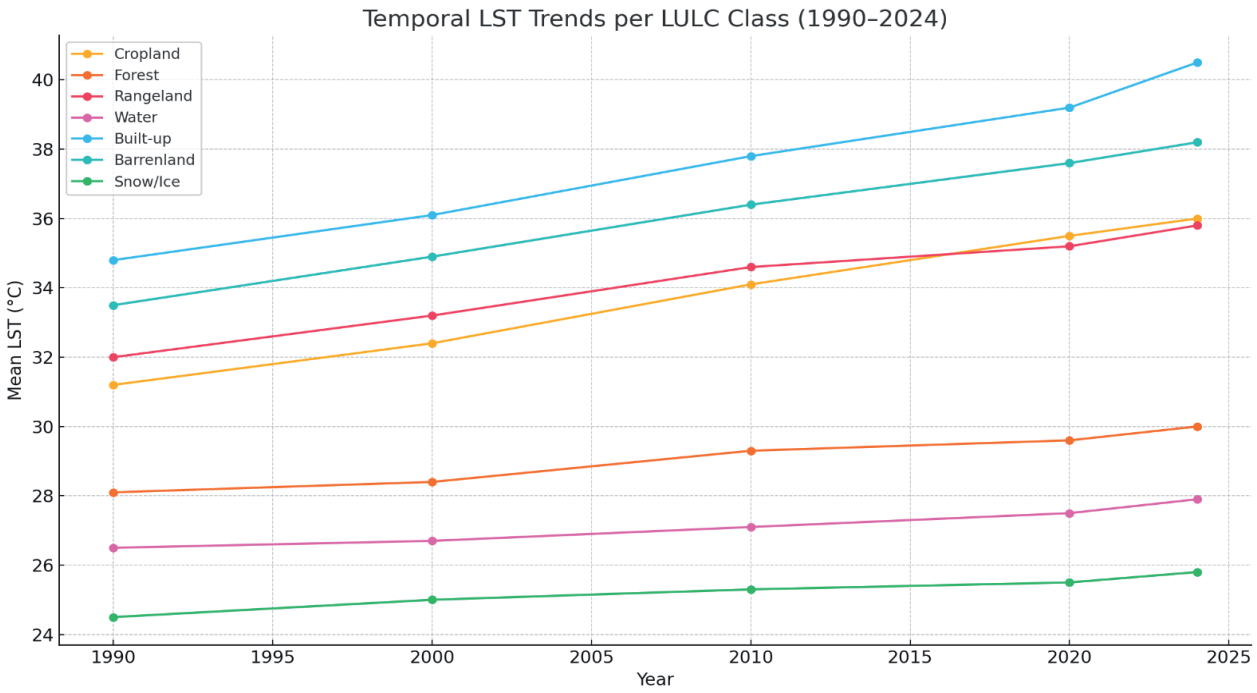

Fig. 7. The graph illustrates the temporal Land Surface Temperature (LST) trends for each LULC class from 1990 to 2024.

consistent coverage and thermal buffering capacity, do not contribute significantly to surface warming and instead act as thermal stabilizers. Similarly, water bodies exhibited a strong positive correlation with LST values, though their absolute LST remained the lowest among all land classes due to their high heat capacity and evaporative cooling effects. The correlation with snow/ice cover was moderate, but due to the very small and stable area of this class, its overall impact on provincial LST patterns is negligible. However, it was included to maintain the completeness of the land classification.

This correlation analysis highly corroborates the hypothesis that LULC alterations, particularly the loss of cropland and increase in built-up land, are strongly linked with increasing LSTs in Henan. The results highlight the important role of land management and urban planning in controlling local climate conditions. Policies like enhancing vegetative cover, maintaining cropland, and encouraging sustainable urban growth could reduce future surface warming in the region.

Discussion

This study set out to examine how land use and land cover (LULC) changes have influenced land surface temperature (LST) in Henan Province over 34 years. The findings show a clear and consistent trend: as urban areas have expanded and cropland has declined, surface temperatures have increased, particularly in areas undergoing rapid land transformation.

These results reinforce the well-documented Urban Heat Island (UHI) effect, where built-up surfaces absorb and retain more heat than vegetated or water-covered areas. In Henan, cities like Zhengzhou and Kaifeng have become prominent thermal hotspots over time, aligning with previous studies that link urban growth to surface heating [16]. The strong positive correlation between built-up land and LST, alongside the negative correlation for cropland and forested areas, highlights the thermal sensitivity of land types to anthropogenic change.

Similar studies in other rapidly urbanizing provinces of China have reported comparable results. For instance, Guangdong and Jiangsu Provinces have shown a clear link between urban expansion and elevated LSTs over the three decades [17, 18]. Comparable findings have also been observed in India and Nigeria, where urban growth and cropland loss intensified the Urban Heat Island (UHI) effect [19, 20]. These consistent patterns highlight that Henan's warming trend is part of a broader global response to urbanization and land cover change.

One of the key mechanisms at play here is the loss of vegetation cover and soil moisture associated with urbanization. When cropland or forest is replaced with concrete, asphalt, or other impervious materials, the land's ability to reflect solar radiation (albedo) and release heat through evapotranspiration drops significantly. As a result, these areas store more heat during the day and release it slowly at night, leading to sustained temperature increases [21].

While forested areas remained relatively stable in Henan, they continued to play an important role in regulating local microclimates. Forests act as thermal buffers due to their canopy structure, higher moisture retention, and cooler surface temperatures [22]. However, their weak statistical correlation with

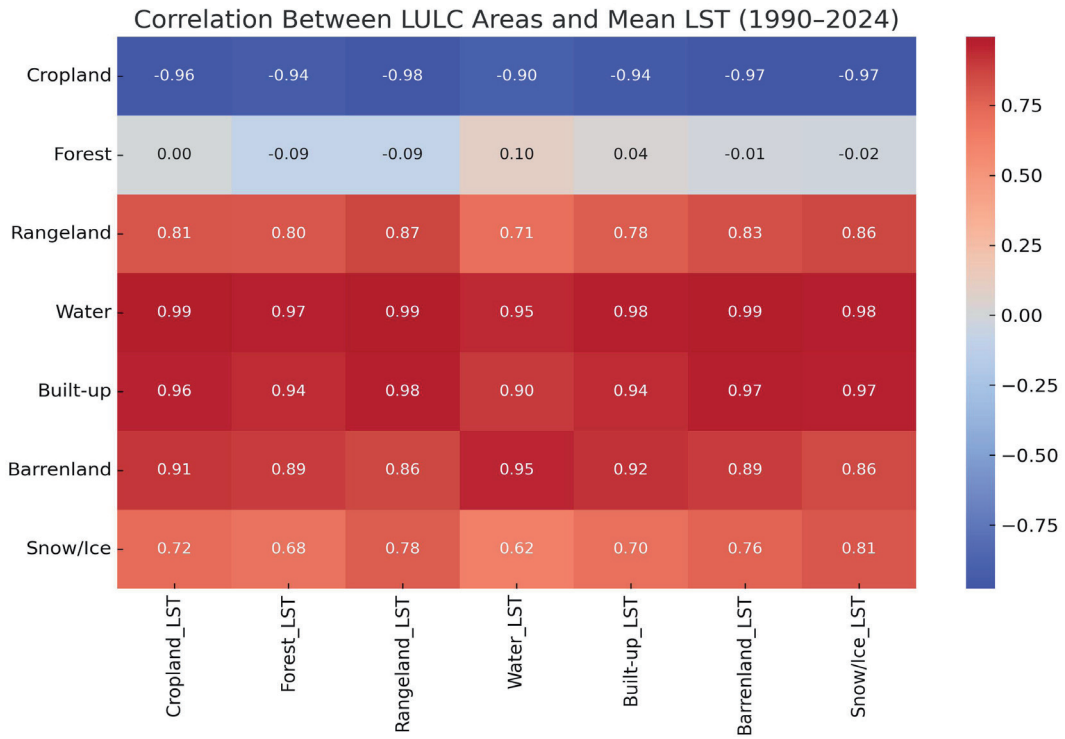

Fig. 8. Correlation between Land Use Land Cover (LULC) area and Mean Land Surface Temperature (LST).

LST in this study likely reflects the fact that forest cover didn't change much in terms of area during the period examined, even though their presence still helps moderate local surface temperatures [23].

Interestingly, water bodies and rangelands also showed dynamic responses. The expansion of water bodies appeared to contribute some local cooling effects, especially in areas close to reservoirs. Rangelands, however, varied more widely, possibly due to shifts in vegetation density and ground exposure [24]. These nuances point to the need for further research into how specific biophysical properties, like vegetation type, soil composition, and seasonal land cover, affect thermal behavior at different scales [25].

Another important consideration is how much of the observed LST rise can be attributed to land cover change versus broader climate change. While our results strongly suggest that urban expansion and land transformation are key drivers of surface warming, it's also likely that Henan has experienced general climatic warming over the past three decades, as reflected in national and global temperature trends [26, 27]. However, the spatial distribution of surface temperature hotspots, closely following urban boundaries, strongly indicates that local land cover change is a major contributor [28].

To isolate these effects further, future work could integrate air temperature data, greenhouse gas trends, or regional climate models [29]. Incorporating nighttime LST and structural equation modeling (SEM) [30] would also help quantify the relative contributions of natural versus human-driven heat inputs. Additionally, including biophysical variables such as forest canopy density, NDVI trends, and land albedo could offer deeper insights into causal mechanisms.

The lack of field validation data is a known limitation of this study. While we cross-checked our LST results with MODIS satellite data and achieved high classification accuracy (Kappa 0.85-0.91), the inclusion of ground-based observations would enhance confidence in the results. We also acknowledge potential uncertainties due to differences among Landsat sensors and assumptions in the LST retrieval process (e.g., emissivity estimation). These challenges are common in large-scale remote sensing studies but should still be taken into account when interpreting results.

Despite these limitations, the findings contribute meaningfully, offering both theoretical and practical insights. Theoretically, the study supports existing models of urban climate change and surface energy balance, while also providing long-term, high-resolution evidence from a Chinese provincial context. Practically, the results highlight the importance of integrating urban planning with environmental management, such as protecting cropland buffers, expanding urban green spaces, and strategically preserving forests.

Conclusions

This study set out to explore how land use and land cover changes have shaped land surface temperature patterns in Henan Province. Using multi-temporal Landsat imagery, cloud-based geospatial tools, and

machine learning classification, we found strong evidence that urban expansion and the decline of cropland have contributed significantly to rising surface temperatures across the region. Built-up areas emerged as the dominant driver of surface heating, with surface temperatures rising most sharply in rapidly urbanizing zones. Conversely, cropland and forested areas helped to regulate temperatures, though their ability to do so weakened where their extent declined. The stable presence of forest, in particular, provided localized cooling benefits, while water bodies also contributed to thermal moderation in nearby areas. While broader climate trends likely played a role in overall warming, the strong spatial alignment between land cover change and LST patterns points to local land transformation as a primary contributor. These findings align with existing research on the Urban Heat Island effect and add valuable long-term, regional insights from one of China's most rapidly developing inland provinces. We acknowledge certain limitations, especially the absence of field validation and the reliance on remote sensing-based assumptions in LST retrieval. Nonetheless, the results offer a reliable and useful foundation for future work. The results underline the importance of better land-use planning to reduce future heat stress. Preserving farmland, maintaining forest cover, and increasing urban green spaces can help to balance development with environmental resilience. Broader climate change is likely adding to these localized warming effects, which makes these strategies even more urgent. Looking ahead, future studies could focus on nighttime temperature patterns, field-based validation, and more detailed socio-economic data to better understand the drivers behind these changes. For policymakers, the message is clear: as Henan and other provinces continue to urbanize, protecting and enhancing natural landscapes will be key to creating cooler, healthier, and more livable cities.

Acknowledgements

The author acknowledges HEBI POLYTECHNIC University for their support.

Conflict of Interest

The authors confirm that no conflicts of interest are associated with the publication of this research. The study was conducted with full independence, ensuring that the design, data collection, analysis, and interpretation were free from any external influence.

References

1. ROY P.S., RAMACHANDRAN R.M., PAUL O., THAKUR P.K., RAVAN S., BEHERA M.D., SARANGI C., KANAWADE V.P. Anthropogenic land use and land cover changes – A review on its environmental consequences and climate change. Journal of the Indian Society of Remote Sensing. **50** (8), 1615, **2022**.
2. IRFEEY A.M.M., CHAU H.-W., SUMAIYA M.M.F., WAI C.Y., MUTTIL N., JAMEI E. Sustainable mitigation strategies for urban heat island effects in urban areas. Sustainability. **15** (14), 10767, **2023**.
3. ZHANG Q., GU L., JIA B., FANG Y. Summertime compound heat extremes change and population heat exposure distribution in China. Journal of Cleaner Production. **485**, 144381, **2024**.
4. KANG S., JIA X., ZHAO Y., LUO M., WANG H., ZHAO M. The Coupling Coordination Relationship Between Urbanization and the Eco-Environment in Resource-Based Cities, Loess Plateau, China. ISPRS International Journal of Geo-Information. **13** (12), **2024**.
5. HALDER B., BANDYOPADHYAY J., BANIK P. Evaluation of the climate change impact on urban heat island based on land surface temperature and geospatial indicators. International Journal of Environmental Research. **15** (5), 819, **2021**.
6. AMMAD WAHEED Q., ZAFEER S., MUHAMMAD Z.-U.-H. Diversity and Distribution of Endemic Flora in Pakistan. Proceedings of the Pakistan Academy of Sciences: B. Life and Environmental Sciences. **60** (2), 165, **2023**.
7. SADIQ KHAN M., ULLAH S., SUN T., REHMAN A.U., CHEN L. Land-use/land-cover changes and its contribution to urban heat Island: A case study of Islamabad, Pakistan. Sustainability. **12** (9), 3861, **2020**.
8. XIN L. Research on Problems and Countermeasures of Agricultural Modernization Development in Henan Province. Academic Journal of Humanities & Social Sciences. **6** (19), 65, **2023**.
9. ZHANG K., MENG H., BA M., WEN D. The Spatial Distribution Characteristics of Resident Population Growth Rate in Henan Province, China. Journal of Geoscience and Environment Protection. **12** (11), 191, **2024**.
10. SARFO I., QIAO J., YEBOAH E., OKRAH A., EL RHADIOUINI C., OSIBO B.K., BOAH A., AMARA D.B. Causal effects and predictin of land use systems in rural landscapes: evidence frm Henan province. Acta Scientiarum Polonorum. Formatio Circumiectus. **23** (3), **2024**.
11. PHAN T.N., KUCH V., LEHNERT L.W. Land cover classification using Google Earth Engine and random forest classifier – The role of image composition. Remote Sensing. **12** (15), 2411, **2020**.
12. GAUR S., MITTAL A., BANDYOPADHYAY A., HOLMAN I., SINGH R. Spatio-temporal analysis of land use and land cover change: a systematic model inter-comparison driven by integrated modelling techniques. International Journal of Remote Sensing. **41** (23), 9229, **2020**.
13. SOUFIANE I.M., DJAOUAD R.D., FARAH B., DJAMEL S. Spatiotemporal Impact of Urbanization on Urban Heat Island Using Landsat Imagery in Oran, Algeria: 1984-2024. Urban Science. **9** (4), 95, **2025**.
14. NJOKU E.A., TENENBAUM D.E. Quantitative assessment of the relationship between land use/land cover (LULC), topographic elevation and land surface temperature (LST) in Ilorin, Nigeria. Remote Sensing Applications: Society and Environment. **27**, 100780, **2022**.
15. QAZI A.W., SAQIB Z., ZAMAN-UL-HAQ M., GARDEZI S.M.H., KHAN A.M., KHAN I., MUNIR A., AHMED I.

Modelling impacts of climate change on habitat suitability of three endemic plant species in Pakistan. Polish Journal of Environmental Studies. **32** (4), 17, **2023**.
16. YAGHOOBI M., VAFAEENEJAD A., MORADI H., HASHEMI H. Analysis of landscape composition and configuration based on LULC change modeling. Sustainability. **14** (20), 13070, **2022**.
17. FU Y., ZHU Z., LIU L., ZHAN W., HE T., SHEN H., ZHAO J., LIU Y., ZHANG H., LIU Z. Remote Sensing Time Series Analysis. Atmosphere. **86**, 91, **2024**.
18. SHI G., YE P., DING L., QUINONES A., LI Y., JIANG N. Spatio-temporal patterns of land use and cover change from 1990 to 2010: A case study of Jiangsu province, China. International Journal of Environmental Research and Public Health. **16** (6), 907, **2019**.
19. ZHAO L., TANG Z.-Y., ZOU X. Mapping the knowledge domain of smart-city research: A bibliometric and scientometric analysis. Sustainability. **11** (23), 6648, **2019**.
20. VINAYAK B., LEE H.S., GEDAM S., LATHA R. Impacts of future urbanization on urban microclimate and thermal comfort over the Mumbai metropolitan region, India. Sustainable Cities and Society. **79**, 103703, **2022**.
21. YI H., ZHANG X., HE L., HE J., TIAN Q., ZOU Y., AN Z. Detecting the impact of the "Grain for Green" program on land use/land cover and hydrological regimes in a watershed of the Chinese Loess Plateau over the next 30 years. Ecological Indicators. **150**, 110181, **2023**.
22. WANG N., NAZ I., ASLAM R.W., QUDDOOS A., SOUFAN W., RAZA D., ISHAQ T., AHMED B. Spatio-temporal dynamics of rangeland transformation using machine learning algorithms and remote sensing data. Rangeland Ecology & Management. **94**, 106, **2024**.
23. REES G., HEBRYN-BAIDY L., BELENOK V. Temporal variations in land surface temperature within an urban ecosystem: A comprehensive assessment of land use and land cover change in Kharkiv, Ukraine. Remote Sensing. **16** (9), 1637, **2024**.
24. WAHLA S.S., KAZMI J.H., TARIQ A. Mapping and monitoring of spatio-temporal land use and land cover changes and relationship with normalized satellite indices and driving factors. Geology, Ecology, and Landscapes. **9** (1), 279, **2025**.
25. GANJIRAD M., BAGHERI H. Google Earth Engine-based mapping of land use and land cover for weather forecast models using Landsat 8 imagery. Ecological Informatics. **80**, 102498, **2024**.
26. ASHRAF T., ASLAM J., MEHMOOD M.S., AHAMAD M.I., REHMAN A. Geospatial assessment of built environment on land surface temperature in district Sheikhupura, Punjab Pakistan. Discover Geoscience. **2** (1), 30, **2024**.
27. BRACHT M.K., OLINGER M.S., KRELLING A.F., GONÇALVES A.R., MELO A.P., LAMBERTS R. Multiple regional climate model projections to assess building thermal performance in Brazil: Understanding the uncertainty. Journal of Building Engineering. **88**, 109248, **2024**.
28. TAMIMINIA H., SALEHI B., MAHDIANPARI M., QUACKENBUSH L., ADELI S., BRISCO B. Google Earth Engine for geo-big data applications: A meta-analysis and systematic review. ISPRS Journal of Photogrammetry and Remote Sensing. **164**, 152, **2020**.
29. QIU H., LI T., ZHANG B. The impact of climate change on the earth system and its simulation predictions: Progress, challenges, and future directions. Geographical Research Bulletin. **3**, 231, **2024**.
30. JAMEI Y., SEYEDMAHMOUDIAN M., JAMEI E., HORAN B., MEKHILEF S., STOJCEVSKI A. Investigating the relationship between land use/land cover change and land surface temperature using Google Earth engine; case study: Melbourne, Australia. Sustainability. **14** (22), 14868, **2022**.